J Radioanal Nucl Chem (2013) 298:813–819
DOI 10.1007/s10967-013-2580-1

Study of size, type and the kerma approximation for thermoluminescent dosimetry

Keyhandokht Karimi-Shahri · Laleh Rafat-Motavalli · Hashem Miri-Hakimabad

Received: 10 January 2013 / Published online: 20 June 2013

Abstract This study aimed to investigate effects of the thermoluminescent dosimeter (TLD) size and type on the absorbed dose value by using of Monte Carlo calculations. The options in creating conditions to establish the kerma approximation were also studied. The Monte Carlo N-Particle (MCNPX 2.4.0) transport code was used to design simulations. Results of this work indicate that if common mineral materials of TLDs are replaced by air and a huge volume is applied for the TLD, the accurate assessment of absorbed doses is possible while the photon energy fluence in the TLD cell is convoluted with mass energy absorption coefficients of the real TLD material. In this method the simulation run-time is strongly decreased.

Keywords Thermoluminescent dosimeters · Kerma approximation · Absorbed dose · Monte Carlo code · ICRP reference voxel phantom

Introduction

Recently, the risk of radiation exposure rises due to increasing use of radiation for a variety of applications. Therefore, finding information about doses received by human body in the different situations, it is crucial.

Thermoluminescent dosimeters (TLDs) are the best instruments to measure the dose and are widely used for radiation detection in the fields of environmental, medical, industrial and personal applications [1–4]. TLDs can be, and commonly are, used for the absorbed dose measurements performed with the aim to investigate cases where dose prediction is difficult and not as part of a routine verification procedure. Among these cases are, for example, new radiotherapies which have been developed for patient treatment during the past decades (e,g. radioimmuno- and boron neutron capture therapies) [5–8]. TLDs have been made from different materials for use in several applications [9, 10]. The main advantages of TLDs are (1) wide useful dose range, (2) small physical size, (3) reusability and therefore, (4) economy, (5) no need for high voltage or cables [11].

Due to the reliance of Monte Carlo codes to do dosimetry calculations nowadays TLDs have been also entered in this method [4, 12, 13]. By using Monte Carlo codes and also anthropomorphic phantoms, for the special applications, and then to do dosimetry calculations can be estimated the dose even before persons are placed in specific situations [14, 15]. The basic point for employing a Monte Carlo code is their ability to provide the accurate estimations within tolerable run-time. Some advantages of TLDs in measurement such small size, mostly $3 \times 3 \times 0.89$ mm^3, are problematic in Monte Carlo simulations. Because in this case, simulations are extremely time-consuming in order to achieve a reasonable statistical accuracy.

The aim of this study was to find a way to carry out simple calculations while have adequate accurate by using TLDs. Calculations are performed for photons in the energies of 0.08, 0.3, 1 and 10 MeV by Monte Carlo N-Particle (MCNPX) code. Lithium fluoride (LiF), calcium fluoride (CaF_2) and calcium sulfate ($CaSO_4$) TLDs were used for calculations. The effect of kerma approximation on obtained doses by TLDs was investigated. TLDs were then wrapped and investigated at different covers. Also LiF TLD was placed on the front- and back surfaces of the

K. Karimi-Shahri · L. Rafat-Motavalli · H. Miri-Hakimabad (✉)
Physics Department, School of Sciences, Ferdowsi University of Mashhad, 91775-1436 Mashhad, Iran
e-mail: mirihakim@ferdowsi.um.ac.ir

ICRP reference voxel phantom to consider the kerma approximation.

Materials and methods

The real volumes of TLDs are very tiny. Therefore, it seems that if the TLD volume is increased, the statistical error and consequently the simulation run-time will be decreased. In other hands, the volume of TLDs should be tiny so that the radiation field is not changed when TLDs are placed on the selected sample. Even the large volume of TLD as an example in personal dosimetry will lead to that it act as a shield for body. A reasonable idea may be found to solve this problem. In present study, investigations using different TLD types and sizes with different MCNPX code tallies were done. Air as a TLD material was also utilized because it has the suitable characteristics; however it is not used in practical applications.

Thermoluminescent dosimeter (TLD)

TLD detectors made from LiF, CaF_2 and $CaSO_4$ were chosen for this study. Several photon energies (0.08, 0.3, 1 and 10 MeV) were selected to cover the typical range of photon energies in medical applications [16, 17]. TLDs were surrounded by the different wrapping materials: polymethyl methacrylate (PMMA: $C_5O_2H_8$), aluminum (Al), polyethylene (CH_2) and polytetrafluoroethylene (Teflon: C_2F_4) in order to establish the kerma approximation. A suitable thickness of the wrapping was calculated for each TLD in certain energies. The effect of thickness, area and volume was investigated on the estimated dose. All changes were done as a homolog.

Calculation procedure

The MCNPX 2.4.0 transport code [18] was used for all calculations. The evaluated nuclear data came from the ENDF/B-VI cross-section library. Four types of MCNPX tallies can be used to estimate the absorbed dose in TLDs. The F6 tally which provides a track length estimate of photon energy deposition in a cell by using kerma approximation in the units of MeV g^{-1} was used. The +F6 tally which gives electron absorbed dose in a cell of same unit with F6 tally was also employed. The *F8 which estimates the amount of total deposited energies in the unit of MeV was also applied. The *F4 tally was used to obtain a track length estimate of photon energy fluence in the cell in MeV cm^{-2} units. Results of this tally should be gathered with dose factor to calculate the collision kerma (K_c). Therefore, the acquired energy spectra in the TLD cell were determined by dE card and mass energy absorption (MEA) coefficients ($\mu_{en}\rho^{-1}$) for type of TLDs was identified by dF card. MEA coefficients came from ICRU [19]. A comparison between these coefficients for the TLD materials used is shown in Fig. 1.

To simulate a broad parallel photon beam, a disk with suitable radius emitting photons in the surface normal vector direction was defined. The statistical errors for all calculations in this study were less than 0.5 %. The calculations here reported for one source photon.

In the part of calculations, male ICRP reference voxel phantom was used. The male phantom is 176 cm in height and 73 kg in weight and the voxel resolution is 2.137 mm × 2.137 mm × 0.8 mm [20]. The phantom includes the all organs and tissues. Additional information about this phantom can be found elsewhere [21, 22]. TLDs are positioned on the chest and back of phantom. Anterior–posterior (AP) and posterior–anterior (PA) irradiation geometries were considered.

Results

Figure 2a–d shows that the absorbed dose increases by the increasing energy. The TLD type also affects the dose values. As an example, obtained doses by LiF TLD are 7 and 6 times lower than from their corresponding values in CaF_2 and $CaSO_4$ TLDs, respectively at 0.08 MeV. These discrepancies are greatly decreased so that the estimated data by LiF TLD are about two times less than obtained values by CaF_2 and $CaSO_4$ TLDs in 0.3–10 MeV.

Figure 2 also presents the effect of TLD thickness on dose values under assumption of the electron equilibrium

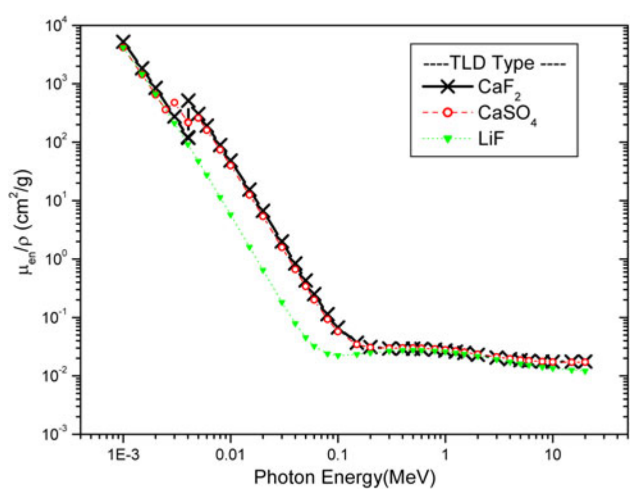

Fig. 1 Comparison of mass energy absorption coefficients for lithium florid (LiF), calcium florid (CaF_2) and calcium sulfate ($CaSO_4$) plotted against photon energy

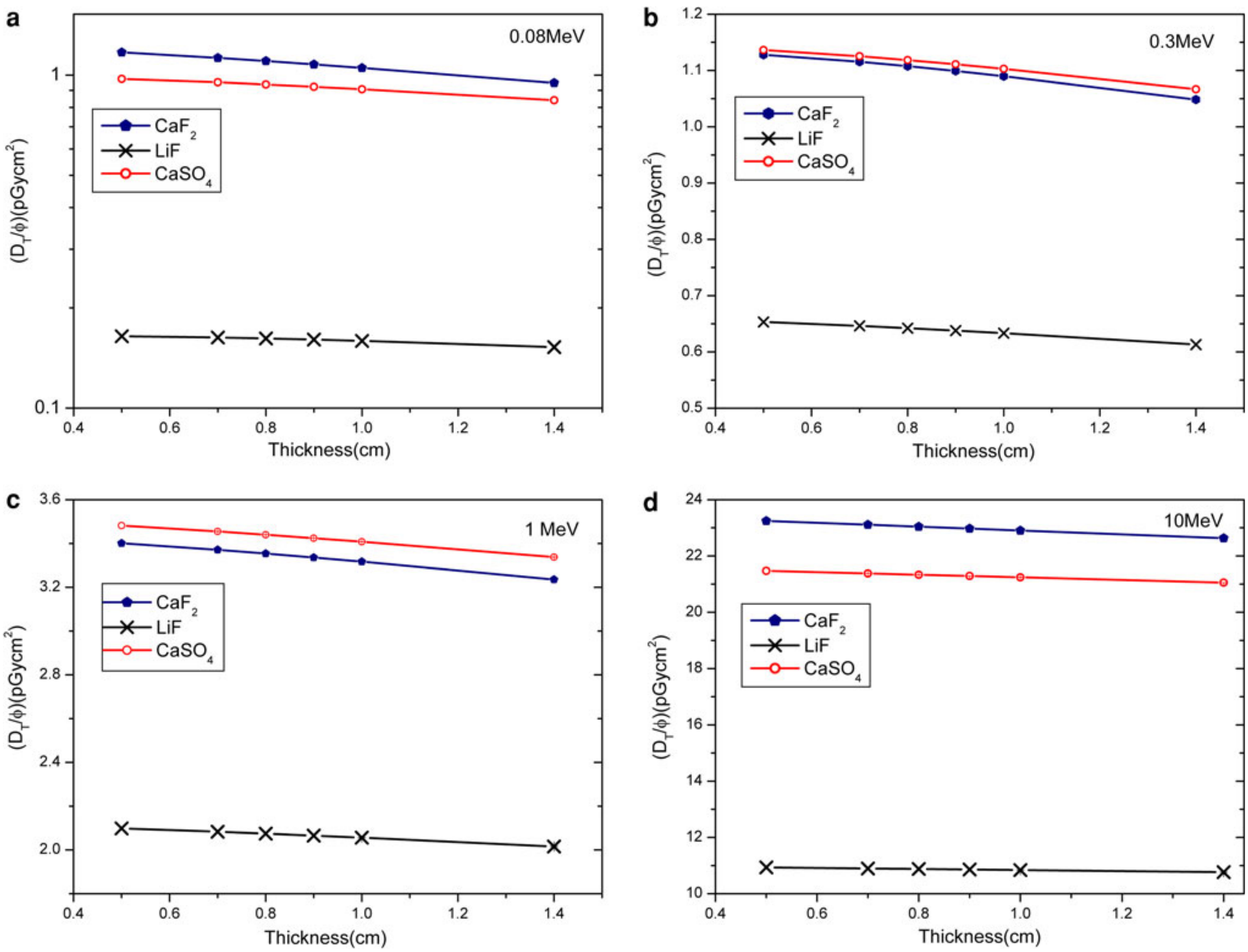

Fig. 2 Absorbed dose per unit fluence in different thicknesses are compared for several energies in the some TLDs

in several selected photon energies; 0.08 MeV (Fig. 2a), 0.3 MeV (Fig. 2b), 1 MeV (Fig. 2c) and 10 MeV (Fig. 2d) using LiF, CaF_2 and $CaSO_4$ TLDs. With increasing thickness of TLD, from 0.5 to 1.4 cm, the photon absorbed dose decreases about 18 %, 6 % and 13 % for LiF, CaF_2 and $CaSO_4$ TLDs, respectively at 0.08 MeV (Fig. 2a). This decrease continues and arrives to 7 %, 6 % and 6 %, respectively in listed TLDs for 0.3 MeV (Fig. 2b). It is clear from Fig. 2c, d that changing of dose is very slow for 1 and 10 MeV and evaluations of the absorbed dose almost remain constant at 10 MeV (2.7 %, 1.4 % and 1.96 % for listed TLDs above). But if the TLD thickness is retained constant and its area is increased, the absorbed dose starts to enlarge. This process is absolutely observed at low energies. The maximum of dose verifications with the area increasing have been indicated in Table 1 for different energies.

In order to investigate the effect of different tallies which able to estimate the dose in the MCNPX code, results of +F6, *F8, F6, *F4 tallies were considered. Figure 3 is a selected graph depicts results for LiF TLD in 0.08 and 1 MeV. In energy of 0.08 MeV, outputs of F6 and *F4 tallies with kerma approximation are completely matched with that of +F6 and *F8 divided by the mass of each TLD. But by increasing photon energies to 1 MeV, results with kerma approximation (F6 and *F4 tallies) are accordance with each other and they are approximately 10 % larger than that of values which have been obtained without kerma approximation (+F6 and *F8 tallies). These differences increase with increasing energy. A similar trend is observed for all TLDs.

Values obtained by considering kerma approximation will be close to those estimated without kerma approximation, if the TLD is surrounded by the different wrapping materials. The role of these TLD walls has been indicated in Table 2. In this table, thicknesses of the wrapping and its corresponding volume at which outputs of F6 tally is consisted with results of +F6 tally, for several energies have been listed. As can be seen with energy increment, required volumes of the wrapping are also increased.

Table 1 The maximum of dose verifications with the area increasing for different energies

TLD types	Energy (MeV)			
	0.08	0.3	1	10
LiF (%)	17	8	3	<1
CaF_2 (%)	21	11	5	<1
$CaSO_4$ (%)	19	9	4	<1

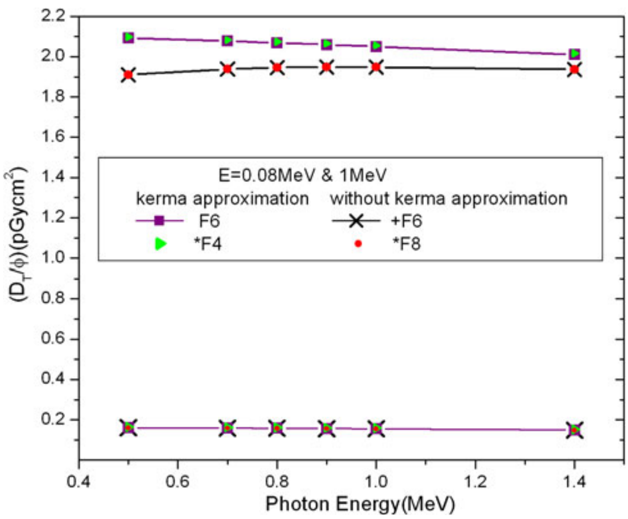

Fig. 3 Comparisons are made between the different type of MCNPX tallies which able to estimate the absorbed dose in LiF TLD for 0.08 and 1 MeV

Another way at which results with and without kerma approximation are consistent with each other, is to place the huge volume in front of TLD. Personal dosimetry was selected for investigation of this subject. One LiF TLD was placed on the chest and the other TLD on the back of male ICRP reference voxel phantom. Figure 4a, b show the response of these TLDs to 25 photon energies ranging from 0.01 to 10 MeV in AP and PA irradiation geometries, respectively. Obtained values from the kerma approximation (F6) and also results without considering the kerma approximation (+F6) were matched together for the back and the front TLD in AP and PA irradiation conditions, respectively. The estimated absorbed dose by +F6 tally is decreased when TLDs are directly exposed for photon energies above 500 keV, such as front TLD in AP irradiation geometry.

We want to find a way at which the dose calculation may be possible for TLD without restriction on the wrapping, type and also the position of TLDs. In the previous suggested way the position of the TLD was limited. As mentioned before, it seems that replacing air instead mineral materials of LiF, CaF_2 and $CaSo_4$ is the suitable suggestion to overcome this problem.

Table 2 The thickness and volume of the different wrapping materials to establish the electron equilibrium in LiF, CaF_2 and $CaSO_4$ TLDs for energies of 0.08, 0.3 and 1 MeV

TLD types	$E = 0.08$ MeV				$E = 0.3$ MeV				$E = 1$ MeV			
	Thickness (cm)/volume (cm^3)				Thickness (cm)/volume (cm^3)				Thickness (cm)/volume (cm^3)			
	Al	PMMA	Polyethylene	Teflon	Al	PMMA	Polyethylene	Teflon	Al	PMMA	Polyethylene	Teflon
LiF	0.309/0.036	0.249/0.159	0.469/0.230	0.145/0.054	0.309/0.036	0.249/0.159	0.469/0.230	0.145/0.054	0.329/0.082	0.4/0.433	0.549/0.351	0.339/0.217
CaF_2	0.330/0.054	0.869/0.556	0.789/0.505	0.389/0.140	0.424/0.068	0.889/0.569	0.820/0.664	0.389/0.140	0.439/0.158	0.889/0.569	0.859/0.727	0.389/0.140
$CaSO_4$	0.459/0.073	0.889/0.569	0.939/0.601	0.399/0.145	0.459/0.073	0.889/0.569	0.949/0.607	0.399/0.145	0.449/0.072	0.899/0.575	0.954/0.614	0.449/0.162

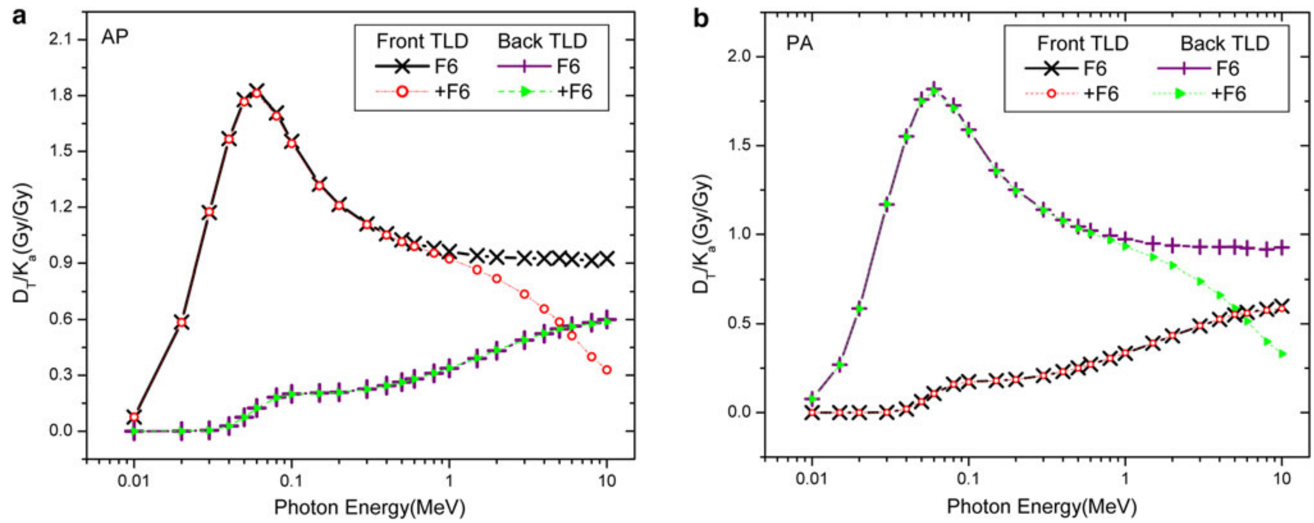

Fig. 4 Comparisons are between LiF TLD responses that are placed on the front and back surfaces of male ICRP reference voxel phantom in AP (**a**) and PA (**b**) irradiation geometries

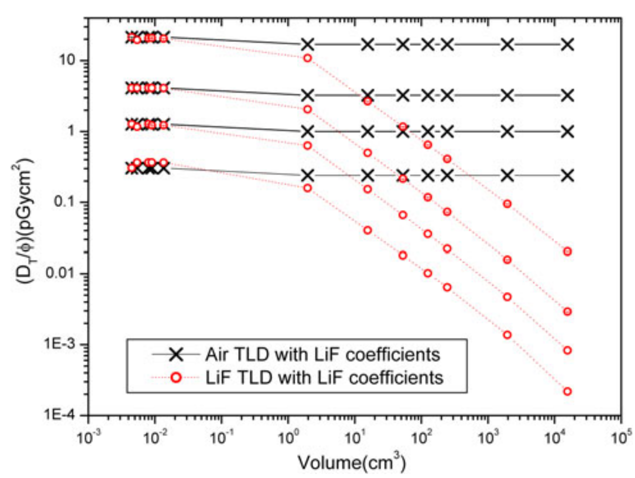

Fig. 5 The estimation of absorbed doses by air and LiF TLDs that the output of *F4 is convoluted with LiF mass energy absorption coefficients for two TLDs

Figure 5 exhibits the results of *F4 tally for air and LiF TLDs which have been convoluted with MEA coefficients of LiF in different volumes of the TLD for 0.08, 0.3, 1 and 10 MeV. The initial volume of TLDs was selected to be 0.004 cm^3 then the volume was increased about 8,000 times rather than the initial volume. It is observable in Fig. 5 that very good agreement is seen between results of air and LiF TLDs in very small volume for all energies. But by increasing volume, the absorbed dose obtained from the LiF TLD is reduced however the acquired dose using the air TLD remains constant. The effect of the thickness and the area on absorbed doses is similar to effect of changing the volume for air TLDs. Similar results are obtained for other TLDs used in this study.

Discussion

Effects of TLD size and type

The probability of particle interaction is high at low energies, thus lead to enhancing the probability of particle capture. However the amount of deposited energy by particles is little and the probability of particle interaction in 1 and 10 MeV is lower than that of 0.08 and 0.3 MeV but the amount of absorbed energies from each interaction is great. For this reason, by increasing energy the absorbed dose is increased.

Estimated doses by the LiF TLD are less than obtained evaluations from the CaF_2 and $CaSO_4$ TLDs in all energies due to the difference in MEA coefficients. Figure 1 illustrates that LiF MEA coefficients are less in compare with two other TLDs data in low energies. In 1 MeV, there is a slight difference between coefficients of listed TLDs. The difference between estimated doses by TLDs is exactly same order with differences between MEA coefficients associated with each TLD. Looking for in detail at MEA coefficients specifies the reason of these discrepancies. For example, in 0.08 MeV which coefficients of CaF_2 are greater than $CaSO_4$ data, photon energies are deposited by photoelectric absorption and Compton scattering. The contribution of Compton for CaF_2 and $CaSO_4$ is same in 0.08 MeV but photoelectric absorptions for these materials are different (photoelectric absorptions is 0.09 and 0.07 $cm^2\ g^{-1}$ for CaF_2 and $CaSO_4$, respectively). Therefore, MEA coefficients for CaF_2 are greater than $CaSO_4$ data.

There is a question as to why doses decrease when the TLD thickness is increased in 0.08 and 0.3 MeV. At low energies (0.08 and 0.3 MeV) the probability of interaction is great thus all of particles are absorbed in a small thickness. By enhancing of the TLD thickness, the number of absorbed particles does not change although, the TLD volume increases. Therefore, the absorbed dose decreases in the TLD. At 1 and 10 MeV by thickness increment, number of absorbed particles also enlarges, so that this increase is relative with volume increasing of the TLD. Accordingly, the thickness changing have not influence on absorbed dose values in these energies.

By increasing the TLD area, number of absorbed particles also increases at low energies that could be due to similar effect of buildup. The particle range increases at high energies thus the increasing area effect could be ignored for these energies.

Kerma approximation

One of the applications of TLDs is to assess the radiation dose received by individual. Since the electron equilibrium exists in the human body, it should be also established in the TLD to create the same conditions. Obviously, in order to consider the electron equilibrium, TLDs were surrounded by the different wrapping materials. Obtained volumes for the TLD wall from various materials is explainable by mass energy attenuation coefficients. Whereas, these coefficients for Teflon are greater than polyethylene, PMMA and Al, the required volume of Teflon for the electron equilibrium creation in the TLD is smaller than listed materials. If a huge volume is placed in front of TLD, the wrapping is not required to establish the electron equilibrium. This idea is well supported by Fig. 4a, b. For the back TLD that body is placed in front of it in AP irradiation geometry and also for the front TLD in PA, the electron equilibrium exists without wrapping.

The effect of different tallies

To take into account how calculation of tallies in MCNPX code, we found that the output of +F6 and *F8 divided by the TLD mass estimate electron absorbed doses while F6 and *F4 tallies assess the kerma. Therefore, it is evident that results of kerma must be consistent with electron absorbed dose values for 0.08 MeV because the kerma approximation is valid for energies lower than 500 keV. But for 1 MeV at which the kerma approximation is invalid, results of the electron absorbed dose are less than kerma values.

The unique characteristic of air is the low density (about 1 mg cm^{-3}). Hence the absorption rarely occurs in it because the probability of photon interactions by Compton scattering, photoelectric absorption and pair production is very low. Therefore, air in compare with mineral materials which is commonly used in the TLD such as LiF, CaF_2 and $CaSO_4$, does not change the incident flux. From Fig. 5 one can deduce that:

$$\varphi_{\text{air}}|_{\text{volume}\ll 1} = \varphi_{\text{TLD}}|_{\text{volume}\ll 1},$$

$$\varphi_{\text{air}}|_{\text{volume}\ll 1} = \varphi_{\text{air}}|_{\text{desired volume}}.$$

This result is contained the interesting and worthy information because by placing the huge volume of the air TLD, the electron equilibrium establishes without using of the wrapping. Subsequently, simulation run-time decreases when the huge volume is applied. Therefore, absorbed doses can be estimated precisely by air TLD which have been made from the huge volume. Then *F4 and MEA coefficients of the desired materials in the real TLD must be applied as the MCNPX output. This result has been recently used by Kim et al. [23]. It is also interesting to note that by using *F4 tally the simulation run-time is about 10 times less than when F6 tally is applied to achieve a reasonable statistical accuracy.

Conclusion

The results of this study indicate that changing the thickness, area and volume of the TLD affects the estimated values of the absorbed dose. Also in common conditions, the TLD should be surrounded by the different wrapping materials with specified volumes or the bulky volume is located in front of TLD to establish the kerma approximation. But other results of the present work revealed that if the air TLD is used even with the huge volume, and then photon energy fluence in the TLD is convoluted with MEA coefficients of the real TLD material can be precisely estimated values of the absorbed dose at all energies.

References

1. German U, Abraham A, Weinstein M, Alfassi ZB (2007) Reassessment of doses in TLD100 by measuring the residual dose. J Radioanal Nucl Chem 273:729–732
2. Kron T (1999) Applications of thermoluminescence dosimetry in medicine. Radiat Prot Dosim 85:333–340
3. Vega-Carrillo HR, Hernandez-Almaraz B (2010) Neutron spectrum and doses in a 18 MeV LINAC. J Radioanal Nucl Chem 283:261–265
4. Eakins JS, Bartlett DT, Hager LG, Tanner RJ (2008) Monte Carlo modeling of a TLD device containing ^{7}LiF:Mg, Cu, P detectors. Radiat Meas 43:631–635
5. Vestad TA, Malinen E, Olsen DR, Hole EO, Sagstuen E (2004) Electron paramagnetic resonance (EPR) dosimetry using lithium formate in radiotherapy: comparison with thermoluminescence (TL) dosimetry using lithium fluoride rods. Phys Med Biol 49:4701
6. Calais PJ, Turner JH (2012) Outpatient ^{131}I-rituximab radioimmunotherapy for non-Hodgkin lymphoma: a study in safety. Clin Nucl Med 37:732–737

7. Savolainen S, Kortesniemi M, Timonen M et al (2012) Boron neutron capture therapy (BNCT) in Finland: technological and physical prospects after 20 years of experiences. Phys Med 29:233–248
8. Liu HM, Liu YH (2011) Error prediction of LiF-TLD used for gamma dose measurement for BNCT. J Appl Radiat Isot 69:1846–1849
9. Espinosa G (2005) Thermoluminescent response of commercial SiO_2 optical fiber to gamma-radiation. J Radioanal Nucl Chem 264:107–111
10. Elisa G, Roberto S, Vando P, Federica F, Giovanni B, Mauro I (2011) Comparison of two different types of LiF:Mg, Cu, P thermoluminescent dosimeters for detection of beta rays (beta-TLDs) from $^{90}Sr/^{90}Y$, ^{85}Kr and ^{147}Pm sources. Health Phys 100:515–522
11. Attix FH (1986) Introduction to radiological physics and radiation dosimetry. Wiley, New York
12. Fernandes AC, Gon IC, Santos J et al (2006) Dosimetry at the Portuguese research reactor using thermoluminescence measurements and Monte Carlo calculations. Radiat Prot Dosim 120:349–353
13. Hranitzky C, Stadtmann H, Olko P (2006) Determination of LiF:Mg, Ti and LiF:Mg, Cu, P TL efficiency for X-rays and their application to Monte Carlo simulations of dosimeter response. Radiat Prot Dosim 119:483–486
14. Zaidi H, Xu XG (2007) Computational anthropomorphic models of the human anatomy: the path to realistic Monte Carlo modeling in radiological sciences. Annu Rev Biomed Eng 9:471–500
15. Johnson PB, Geyer A, Borrego D, Ficarrotta K (2011) The impact of anthropometric patient-phantom matching on organ dose: a hybrid phantom study for fluoroscopy guided interventions. Med Phys 38:1008–1017
16. Kron T (1994) Thermoluminescence dosimetry and its applications in medicine—Part 1: physics, materials and equipment. Australas Phys Eng Sci Med 17:175–199
17. Kron T (1994) Thermoluminescence dosimetry and its applications in medicine—Part 2: history and applications. Australas Phys Eng Sci Med 17:175–199
18. Waters L (2002) MCNPX^{TM} user's manual, version 2.4.0. Report LACP-02-408. Los Alamos National Laboratory
19. ICRU (1989) Tissue substitutes in radiation dosimetry and measurement. Report 44 of the International Commission on Radiation Units and Measurements, Bethesda
20. Xu XG, Eckerman KF (2010) The ICRP reference computational phantoms. In: Handbook of anatomical models for radiation dosimetry, 1st edn. CRC Press, New York
21. ICRP (2003) Basic anatomical and physiological data for use in radiological protection: reference values. ICRP Publication 89. Pergamon Press, Oxford
22. IRCP (2009) Adult reference computational phantoms. ICRP Publication 110. International Commission of Radiological Protection. Elsevier, Amsterdam
23. Kim CH, Cho S, Jeong JH, Bolch WE, Reece WD, Poston JW Sr (2011) Development of new two-dosimeter algorithm for effective dose in ICRP Publication 103. Health Phys 100:462–467